

Harmonic generation in a two dimensional nonlinear quasicrystal

R. T. Bratfalean, A.C. Peacock, N. G. R. Broderick,* and K. Gallo

Optoelectronics Research Centre, University of Southampton, Southampton, SO17 1BJ UK

Ruth Lewen

Electronics and Computer Science, University of Southampton, Southampton, SO17 1BJ UK

Abstract

Second harmonic generation in a two dimensional nonlinear quasi-crystal is demonstrated for the first time. Temperature and wavelength tuning of the crystal reveal the uniformity of the pattern while angle tuning reveals the dense nature of the crystal's Fourier spectrum. These results compare well with theoretical predictions showing the excellent uniformity of the crystal and suggest that more complicated "nonlinear holograms" should be possible.

Periodic poling of ferroelectric materials such as lithium niobate is a well established technique for improving the efficiency of nonlinear optical processes[1]. When combined with channel waveguide technology, periodically poled lithium niobate (PPLN) is perhaps the premier system for nonlinear optics at telecommunications wavelengths. Recently work has begun in exploring both theoretically[2, 3] and experimentally[4, 5] the properties of two dimensionally poled nonlinear photonic crystals. We present here the first example of a two dimensionally poled nonlinear quasi-crystal and discuss its properties.

The importance of a PPLN crystal can best be understood by considering second harmonic generation (SHG). In this process two photons of frequency ω_1 are converted into one photon of frequency $2\omega_1$ a process that automatically conserves energy. For this interaction to occur momentum must also be conserved leading to:

$$\mathbf{k}(\omega) + \mathbf{k}(\omega) + \mathbf{G}_n = \mathbf{k}(2\omega) \quad (1)$$

where \mathbf{k} is the wavevector of the light in the material and \mathbf{G}_n is a reciprocal lattice vector of the crystal. For a strictly periodic PPLN crystal $|\mathbf{G}_n| \propto n/d$ where $n \in \mathbb{Z}$ and d is the period of the crystal. As the period of the crystal can be freely chosen during the fabrication process, Eq. (1) is also a design rule for PPLN allowing the phase matching of any *single* interaction.

If we consider a harder problem that of simultaneously phase matching two nonlinear processes we can immediately see that instead of having to satisfy one momentum conservation equation we need to satisfy two. With the only free parameter in a PPLN crystal being the domain period d this cannot in general be done as the phase mismatches are rarely integer multiples of some constant. Hence an alternative approach must be taken. The simplest scheme would be to write two gratings on top of one another, however due to the digital nature of the poling process (essentially the nonlinear coefficient can be either ± 1) and the fact that there is a minimum domain size of $\approx 5\mu\text{m}$, means that this is not possible and more complicated patterns must be poled. Two different patterns have been suggested in the literature. The first is to use an aperiodic pattern usually based on a Fibonacci sequence[6] while the second is to use a two dimensional periodic pattern[7]. Our aim in this paper is to look at the combination of both approaches, i.e. a two dimensional aperiodic poled pattern.

More generally there is a need to produce poled patterns that are not strictly periodic such as chirped PPLN, superstructured PPLN, transversed pattern PPLN etc[8, 9, 10]. In all these cases the additional structure in real space provides additional functionality (e.g. pulse compression, spatial focussing, etc.) and we can consider these gratings as simple cases of “nonlinear holography”

in which both the temporal and frequency components of an input pulse are altered to produce an output pulse with both a different central frequency and pulse shape. Doing this in an arbitrary fashion would require the ability to pole arbitrary shapes in a 2D crystal and as a stepping stone we look in this paper at the poling and optical response of a 2D Penrose pattern as shown in Fig. 1.

A Penrose pattern is an aperiodic tiling of the plane which has long range order but which lacks any translational or rotational symmetry[11]. As shown in Fig. 1, a Penrose pattern can be thought of as a tiling of a plane by two rhombuses - a “thick” rhombus and a “thin” rhombus. To go from the Penrose lattice to our crystal structure we decided to place a poled region at each vertex point (the alternative of placing a poled region at the centre of each rhombus was considered and makes no significant difference). Upon taking the Fourier transform of the resulting structure the result is as shown in Fig. 1 (insert). In the insert the location of the dots correspond to the location of reciprocal lattice vectors which can be used for quasi-phase matching [via Eq. (1)] while the size of the dots indicate the size of the corresponding Fourier coefficients.

As there are an infinite number of nonequivalent Penrose tilings of the plane[12] (two tilings are nonequivalent if one cannot be transformed into the other by a simple translation and rotation) it was necessary to decide which one to use. Clearly initially the pattern must be scaled so that the reciprocal lattice vectors satisfy Eq. (1). Then the size and the shape of the poled regions must be chosen to maximum the relevant Fourier coefficient (in a QPM process the strength of the interaction is proportional to the size of the Fourier coefficient corresponding to the reciprocal lattice vector mediating the process). We numerically generated several different patterns and optimised the shape of the poled region resulting in a pattern that could be used to phase match second harmonic generation at 140° C with a fundamental wavelength of 1536nm.

We then wrote a 20.53mm by 1.15mm portion of this Penrose pattern onto a lithography mask which was used to pole the LiNbO₃ crystal in the standard way. A thin layer of photo-resist was deposited on the -z face of the 0.5mm thick, z-cut LiNbO₃ sample and then photo-lithographically patterned according to the mask. The width and lengths of the Penrose regions were carefully aligned with the x and y crystallographic axes of LiNbO₃ , respectively. Poling was accomplished by applying an electric field via liquid electrodes on the $\pm z$ faces at room temperature. As shown in Fig. 1, the Penrose pattern fabricated onto the sample was found to be uniform across the entire poled area and was faithfully reproduced throughout the crystal depth (z axis). Finally we polished the $\pm x$ faces, allowing a propagation length of 20mm through the sample.

We first measured the temperature tuning curve for second harmonic generation. The crystal was rotated with respect to the incident beam to obtain maximum SHG at 140°C. Next the

temperature tuning curve was measured over the range $120 - 160^{\circ}\text{C}$ as shown in Fig. 2 and has a FWHM of 5.1°C . For this measurement the incident fundamental beam was gently focussed into the crystal and consisted of 5 ns pulses at a repetition rate of 100 kHz and an average power of 300 mW which was sufficiently small to ensure we were in the low conversion regime. The input beam was confocally focused to a spot size of $162\text{ }\mu\text{m}$ in the centre of the crystal. Due to non-collinear nature of the interaction we would expect a Gaussian response rather than a sinc shaped one[13] and that it should be broader than a collinear response.

Next we measured the wavelength response of the crystal over the range 1533nm to 1543nm using a tuneable source with an average power of 150mW. The crystal was rotated to give maximum SHG at 1538nm and kept at a constant temperature of 140°C . The results are as shown in Fig. 2 (insert). We found a FWHM of 1.3nm which corresponds well to the measured temperature tuning width.

A distinguishing feature of an aperiodic crystal compared to a periodic crystal is the dense nature of its Fourier transform. As such it should be possible to observe SHG with our crystal for a much larger set of input angles than for a periodic crystal (see Fig. 4 in [4]). To do this we fixed the input wavelength and incident power and the crystal temperature and rotated the crystal noting when a SH spot appeared. For each SH beam that was produced we measured the input angle of the fundamental along with the angle between the fundamental and second harmonic. These results are shown in Fig. 3 (circles). We measured 43 distinct spots which was roughly 50% more than what we had measured previously for a periodic crystal (the numbers are not strictly comparable as the input power was roughly 1000 times bigger in the earlier measurement[4]!) illustrating the dense nature of the Fourier space. In addition we have shown on Fig. 3 the theoretically predicted input and output angles for the Fourier peaks involved in the interactions.

The importance of measuring the output SHG spots is that it directly gives us information about the position and strength of the peaks in Fourier space which in turn gives us information about the crystal lattice. For example Fig. 3 is mirror symmetric to a good degree indicating a mirror plane in Fourier space. We were not however able to rotate the crystal sufficiently to observe fully the 5 fold symmetry but the beginnings of it can be seen. We are able to account for almost all of the experimental spots apart from two while similarly only one theoretical Fourier peak appears for which there is no corresponding experimental spot. The reason for this is not currently known although we believe that it might relate to overpoling of the crystal in some regions causing a change in the size of the Fourier coefficients.

Finally we measured the efficiency of the second harmonic generation for near normal incidence

and at a temperature of 105° C. The reason for this is that while angle tuning of the crystal gives us information about the location of the peaks in Fourier space it does not provide us with any information about their size. However the SH power is proportional to the square of the Fourier coefficients which in turn depends on the size of the poled regions. For the spot we chose we measured an efficiency of 1.64% while the predicted theoretical efficiency for a collinear interaction would be 2.73%. The two most likely causes for this discrepancy are the noncollinear nature of our interaction which would reduce the efficiency and the fact that we do not precisely know the size of the poled regions over the whole of the crystal. Thus our measurements suggest that there is some degree of overpoling in the crystal. We note that although the efficiency is low this is due to the choice of Fourier peak choosing a different Fourier peak should in principle allow conversion efficiencies > 90% for our available pump power.

In conclusion we have designed and fabricated the first two dimensional nonlinear photonic quasicrystal for use in second harmonic generation. Measurements on this crystal demonstrate the greater density of reciprocal lattice vectors compared to a periodic crystal along with the five fold rotational symmetry. Such crystals are likely to find use in the simultaneous phase-matching of multiple nonlinear interactions due to their flexibility in the location of the Fourier peaks. The fabrication of such a non-periodic crystal is a significant step forwards towards the design and fabrication of "nonlinear holograms" which would allow complete spatial and temporal shaping of input beams through the nonlinearity.

* Electronic address: ngb@orc.soton.ac.uk

- [1] J. A. Armstrong, N. Bloembergen, J. Ducuing, and P. S. Pershan, "Interactions between Light Waves in a Nonlinear Dielectric," *Phys. Rev.* **127**, 1918 (1962).
- [2] V. Berger, "Nonlinear Photonic Crystals," *Phys. Rev. Lett.* **81**, 4136–4139 (1998).
- [3] A. H. Norton and C. M. de Sterke, "Optimal poling of nonlinear photonic crystals for frequency conversion," *Opt. Lett.* **28**, 188–190 (2003).
- [4] N. G. R. Broderick, G. W. Ross, H. L. Offerhaus, D. J. Richardson, and D. C. Hanna, "HeXLN: A two dimensional nonlinear photonic crystal," *Phys. Rev. Lett.* **84**, 4345–4348 (2000).
- [5] A. Chowdhury, C. Staus, B. F. Boland, T. F. Kuech, and L. McCaughan, "Experimental demonstration of 1535-1555-nm simultaneous optical wavelength interchange with a nonlinear photonic crystal," *Opt. Lett.* **26**, 1353–1355 (2001).
- [6] S. ning Zhu, Y. yuan Zhu, Y. qiang Qin, H. feng Weng, C. zhen Ge, and N. ben Ming, "Experimental Realization of Second Harmonic Generation in a Fibonacci Optical Superlattice of LiTaO₃," *Phys. Rev.*

- Lett. **78**, 2752–2755 (1997).
- [7] S. M. Saltiel and Y. S. Kivshar, “Phase matching in nonlinear $\chi^{(2)}$ photonic crystals,” Opt. Lett. **25**, 1204–1206 (2000).
 - [8] G. Imeshev, M. A. Arbore, M. M. Fejer, A. Galvanauskas, M. Fermann, and D. Harter, “Ultra-short pulse second harmonic generation with longitudinally nonuniform quasi-phase-matching gratings: pulse compression and shapping,” J. Opt. Soc. Am. B **17**, 304–318 (2000).
 - [9] G. Imeshev, M. Proctor, and M. M. Fejer, “Lateral patterning of nonlinear frequency conversion with transversely varying quasi-phase-matching gratings,” Opt. Lett. **23**, 673–675 (1998).
 - [10] J. R. Kurz, A. M. Schober, D. S. Hum, A. J. Saltzman, and M. M. Fejer, “Nonlinear physical optics with transversely patterned quasi-phase-matching gratings,” IEEE J. Select. Top. Quantum Electron. **8**, 660–664 (2002).
 - [11] R. Penrose, “The Role of Aesthetics in Pure and Applied Mathematical Research,” in *The Physics of Quasicrystals*, P. J. Steinhardt and S. Ostund, eds., (World Scientific, Singapore, 1987), Chap. Appendix I.
 - [12] D. Levine and P. J. Steinhardt, “Quasicrystals. I. Definition and Structure,” Phys. Rev. B **34**, 596–616 (1986).
 - [13] N. G. R. Broderick, R. T. Bratfalean, T. M. Monco, D. J. Richardson, and C. M. de Sterke, “Temperature and wavelength tuning of 2nd, 3rd and 4th harmonic generation in a two dimensional hexagonally poled nonlinear crystal,” J. Opt. Soc. Am. B **19**, 2263–2272 (2002).

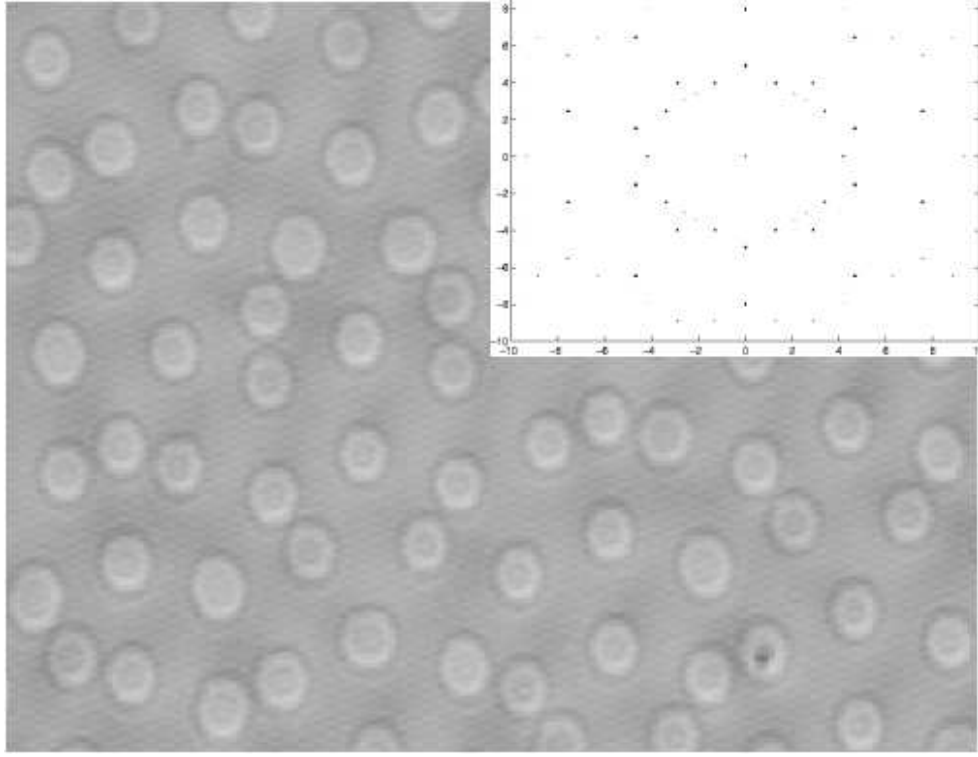


FIG. 1: Optical picture of the poled pattern used in the experiments. The insert shows the Fourier transform of the pattern.

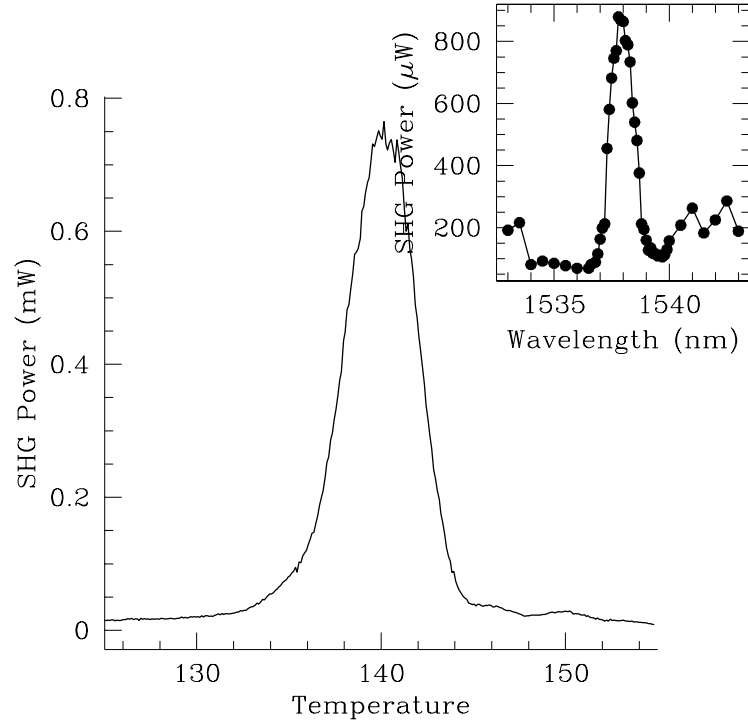


FIG. 2: Temperature Tuning curve for the Penrose Pattern. The insert shows the wavelength tuning response.

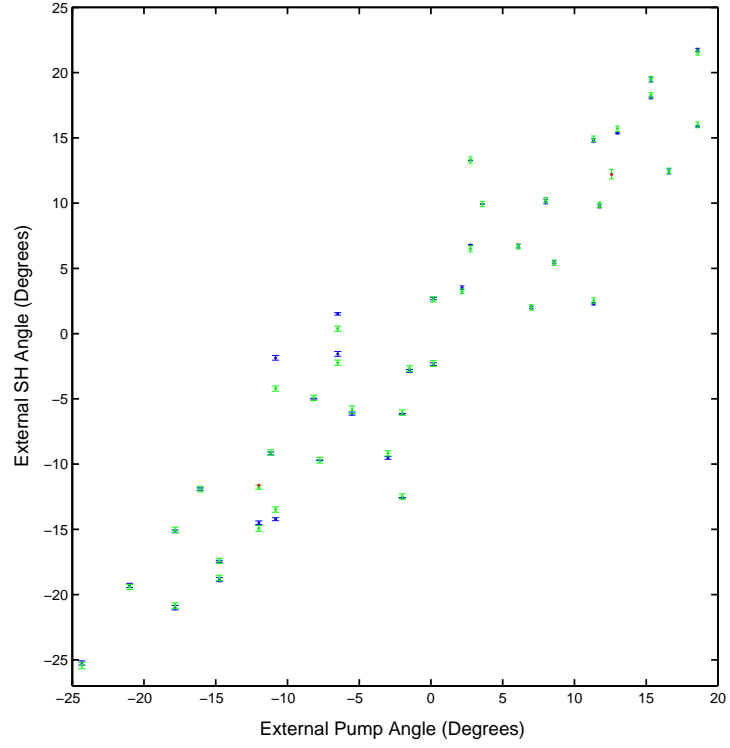


FIG. 3: Picture of the measured and theoretical input and output angles for the Penrose pattern.